Geophysical Research Letters

RESEARCH LETTER
10.1029/2018GL078127

Key Points:
- Microbial and fossil fuel sources of CH_4 have both contributed to the observed increase in atmospheric CH_4 from 2007
- Fossil fuel sources of CH_4 decreased significantly between 1990 and 1996 but increased again from the early 2000s
- Variation in the main atmospheric sink of CH_4, oxidation by OH radicals, appears not to have significantly contributed to the recent increase in CH_4

Supporting Information:
- Supporting Information S1

Correspondence to:
R. L. Thompson,
rona.thompson@nilu.no

Citation:
Thompson, R. L., Nisbet, E. G., Pisso, I., Stohl, A., Blake, D., Dlugokencky, E. J., et al. (2018). Variability in atmospheric methane from fossil fuel and microbial sources over the last three decades. *Geophysical Research Letters*, *45*, 11,499–11,508. https://doi.org/10.1029/2018GL078127

Received 29 MAR 2018
Accepted 3 OCT 2018
Accepted article online 10 OCT 2018
Published online 20 OCT 2018

Variability in Atmospheric Methane From Fossil Fuel and Microbial Sources Over the Last Three Decades

R. L. Thompson[1], E. G. Nisbet[2], I. Pisso[1], A. Stohl[1], D. Blake[3], E. J. Dlugokencky[4], D. Helmig[5], and J. W. C. White[5]

[1]Norwegian Institute for Air Research (NILU), Kjeller, Norway, [2]Department of Earth Sciences, Royal Holloway University of London (RHUL), London, UK, [3]Department of Chemistry, University of California Irvine (UCI), Irvine, CA, USA, [4]Global Monitoring Division, National Oceanic and Atmospheric Association, Silver Spring, MD, USA, [5]Institute of Arctic and Alpine Research (INSTAAR), University of Colorado, Boulder, CO, USA

Abstract Atmospheric measurements show an increase in CH_4 from the 1980s to 1998 followed by a period of near-zero growth until 2007. However, from 2007, CH_4 has increased again. Understanding the variability in CH_4 is critical for climate prediction and climate change mitigation. We examine the role of CH_4 sources and the dominant CH_4 sink, oxidation by the hydroxyl radical (OH), in atmospheric CH_4 variability over the past three decades using observations of CH_4, C_2H_6, and $\delta^{13}C_{CH4}$ in an inversion. From 2006 to 2014, microbial and fossil fuel emissions increased by 36 ± 12 and 15 ± 8 Tg y^{-1}, respectively. Emission increases were partially offset by a decrease in biomass burning of 3 ± 2 Tg y^{-1} and increase in soil oxidation of 5 ± 6 Tg y^{-1}. A change in the atmospheric sink did not appear to be a significant factor in the recent growth of CH_4.

Plain Language Summary Methane is the second most important greenhouse gas and is responsible for approximately 17% of the direct radiative forcing from all long-lived greenhouse gases. Observations of methane in the atmosphere have shown a dramatic increase from 2007 after a period of relative stability between the late 1990s and early 2000s, but the cause of this increase is still under scientific debate. This study uses atmospheric observations of methane and two related tracers, the isotopic ratio of carbon in methane and ethane, to constrain the sources and sinks of methane over the past three decades. The increase in methane between 2007 and 2014 is likely due to an increase in microbial sources, of 24–48 Tg/y (predominantly natural wetlands and agricultural), as well as fossil fuel sources, of 7–23 Tg/y. In contrast to other recent studies, a reduction in the atmospheric sink of methane was found not to be a significant factor in explaining the recent atmospheric increase.

1. Introduction

Atmospheric methane (CH_4) grew throughout the 20th century, from ~880 nmol mol^{-1} (or parts per billion, ppb) in 1900 (Etheridge et al., 1998) to ~1,750 ppb in 1999 (Dlugokencky et al., 2003) based on measurements in the remote marine boundary layer. The increase was largely due to human activities, particularly the extraction, transport and storage of fossil fuels, and agriculture (Ciais et al., 2013). On top of this predominantly increasing trend are significant interannual and decadal variations. The most pertinent of these since the late 20th century are a decrease in the growth rate from the mid 1980s to late 1990s, a period of little growth between 1999 to 2007, and a significant CH_4 increase from 2007 (Nisbet et al., 2014, 2016). Despite the importance of these changes for climate scenarios and emission mitigation, their causes are not well understood owing to the large uncertainties in the sources, anthropogenic and natural, as well as the primary sink, that is, oxidation by the hydroxyl radical (OH) in the atmosphere.

A number of recent studies have sought to improve understanding of CH_4 variability using box models or 3-D atmospheric transport models to compare different source and sink scenarios with atmospheric observations (Kirschke et al., 2013; Nisbet et al., 2016; Rice et al., 2016; Rigby et al., 2017; Saunois et al., 2017; Schaefer et al., 2016; Schwietzke et al., 2016; Turner et al., 2017). As observations of atmospheric CH_4 alone do not provide a sufficient constraint to resolve the sources and sinks, these studies have used the additional information given by the change in the ^{13}C:^{12}C ratio in atmospheric CH_4 (recorded as the change with respect to a standard ratio with the notation $\delta^{13}C_{CH4}$ and in units of per mil or ‰; Nisbet et al., 2016). Microbial sources, such as wetlands, enteric fermentation in ruminant animals, and landfills, are relatively depleted in ^{13}C (more

negative $\delta^{13}C_{CH4}$), while thermogenic sources, such as fugitive emissions from fossil fuels, natural gas seepage, and biomass burning (especially of tropical grasslands), are relatively rich in ^{13}C (less negative $\delta^{13}C_{CH4}$; Dlugokencky et al., 2011).

Even with the additional information from $\delta^{13}C_{CH4}$, these studies have found contradicting explanations for the variability in atmospheric CH_4. For example, the observed increase in CH_4 from 2007, and the accompanying decrease in $\delta^{13}C_{CH4}$, has been interpreted in a few studies as an indication of an increase in microbial sources, particularly subtropical and tropical wetlands and agriculture (Nisbet et al., 2016; Schaefer et al., 2016). In contrast, other recent studies have highlighted that the observations may also be explained by a decrease in the OH sink of CH_4 with little or no change in the sources, since OH preferentially oxidizes $^{12}CH_4$ (Rigby et al., 2017; Turner et al., 2017). However, these studies only infer changes in OH indirectly and it is unclear what would cause a decrease in the OH sink of the magnitude required to explain the trends in CH_4 and $\delta^{13}C_{CH4}$. Moreover, if the oxidative capacity of the atmosphere has declined, the consequences should be seen on other atmospheric species and not just on CH_4. In fact, there is evidence to suggest that the OH sink of CH_4 may have increased as a result of a decrease in the atmospheric abundance of CO (Gaubert et al., 2017). In another study it was suggested that biomass burning (a ^{13}C-rich source of CH_4) has decreased from 2007 and may have masked an increase in fossil fuel emissions with an overall small decrease in $\delta^{13}C_{CH4}$ in the global source (Worden et al., 2017). Given the change in biomass burning, Worden et al. (2017) propose that the most likely scenario to explain the CH_4 and $\delta^{13}C_{CH4}$ trends from 2007 is an increase in both fossil fuel and microbial emissions.

Owing to the persisting ambiguities in the sources and sinks, even when using both CH_4 and $\delta^{13}C_{CH4}$ observations, additional atmospheric tracers have been proposed. For instance, methylchloroform has been used to help constrain the OH sink (Montzka et al., 2011). However, since errors in methylchloroform emissions are folded into the estimates of OH, these consequently also affect estimates of the CH_4 source (Krol et al., 2005). This problem has been exacerbated by the fact that methylchloroform emissions and atmospheric mixing ratios have now reached low levels, thus increasing the relative uncertainties (Liang et al., 2017). Also, it cannot be ruled out that emissions of methylchloroform may be significantly underestimated with large sources going undetected, as was the case for CFC-11 (Montzka et al., 2018). The D:H isotope ratio in CH_4, δD_{CH4}, has also been used similarly to $\delta^{13}C_{CH4}$ to help constrain the sources and sinks (Rice et al., 2016); however, δD_{CH4} measurements are very sparse.

In this study, we use ethane (C_2H_6) as an additional tracer to constrain the sources and sinks of CH_4. Ethane is co-emitted with CH_4 by fossil fuel extraction and distribution (Kort et al., 2016; Smith et al., 2015) as well as in natural gas seepage from land (Etiope & Ciccioli, 2009) and is a particularly interesting tracer as its other sources are relatively minor, that is, biomass burning and marine seeps (Etiope & Ciccioli, 2009). In addition, C_2H_6 is also primarily lost via OH oxidation (Rudolph, 1995) with the result that changes in OH will affect both CH_4 and C_2H_6 in a similar way. A further advantage of C_2H_6 is that observations are available from discrete samples (flasks) at a multitude of sites globally since the early 1980s. Ethane levels in the atmosphere decreased from 1984 to 2009, leading to the hypothesis that the decline in CH_4 growth rate around the same time was at least partly due to a reduction in fossil fuel sources (Simpson et al., 2012). More recently, C_2H_6 levels at Northern Hemisphere (NH) sites have risen again leading to speculation that fossil fuel emissions have increased and have contributed to the recent increase in CH_4 (Hausmann et al., 2016; Helmig et al., 2016), although an increase in fossil fuel emissions alone is inconsistent with the observed negative trend in $\delta^{13}C_{CH4}$.

Here we exploit C_2H_6, in addition to CH_4 and $\delta^{13}C_{CH4}$, in a formal statistical optimization to estimate the sources and atmospheric sink of CH_4 and to determine the primary causes of atmospheric variation over the period of 1980 to 2014.

2. Methodology

We use a Bayesian atmospheric inversion to optimize the sources and the OH sink to best match observations of CH_4, $\delta^{13}C_{CH4}$, and C_2H_6 within the uncertainty ranges of the observations, prior emissions, and prior sinks. Atmospheric chemistry and transport were calculated using the AGAGE 2-D model of the atmosphere, which is suited to the focus on multiannual trends because of its computational efficiency. This model has four

equal area boxes in the latitudinal direction and three vertical layers representing the lower troposphere, upper troposphere, and stratosphere (Cunnold et al., 2002). We adapted the AGAGE model to compute monthly CH_4 and C_2H_6 mixing ratios and changes in $\delta^{13}C_{CH4}$ based on sources and the sinks due to reactions with OH and Cl (for details see Text S1 and Tables S1–S4 in the supporting information).

Emissions of CH_4 were grouped into six categories based on their $\delta^{13}C_{CH4}$ values: microbial (including wetlands, rice cultivation, enteric fermentation, and termites with a mean value of -63.2 ± 0.8‰), fugitive emissions from fossil fuel (including natural gas seepage from land, -40.0 ± 1.0‰), landfills (-55.6 ± 0.7‰), biomass burning (-22.2 ± 1.9‰), ocean (assumed to have no effect on $\delta^{13}C_{CH4}$), and soil oxidation (a negative emission to the atmosphere, -19.7 ± 2.9‰). The $\delta^{13}C_{CH4}$ values for each of the six CH_4 source categories were based on literature values and are summarized in Text S2 and Table S4. Atmospheric loss of CH_4 by OH and Cl oxidation is also associated with a kinetic isotope effect; for OH we used -4.7 ± 0.7‰ and for Cl -61.9 ± 1.0‰ (Table S4). Although the total loss due to Cl oxidation is relatively small, with estimates ranging from 12 to 37 Tg y^{-1} (Allan et al., 2007; Hossaini et al., 2016), the resulting ^{13}C enrichment is significant but has previously not been considered in inversions for CH_4.

Emissions of C_2H_6 were grouped into two categories: fugitive emissions from fossil fuel (including natural gas seepage from land) and other emissions (including biomass burning and ocean sources). The fugitive emissions of CH_4 and C_2H_6 were related to one another by an ethane to methane mass emission ratio of 0.15 ± 0.025. This ratio was calculated as the weighted average of observed emission ratios for coal, 0.19 (Strępoć et al., 2007), oil and gas, 0.33 and 0.09, respectively (Jones et al., 1999) with a weighting by the relative contribution of coal, oil and gas to the total fossil fuel CH_4 source based on the data set of Schwietzke et al. (2014). Using this data set, no significant trend in the ratio was found from 1980 to 2011 (the period covered by the data) at the scale of the latitudinal boxes. It is still possible though that the actual ratio has varied, especially more recently owing to the changing importance of nonconventional versus conventional sources of natural gas and oil, particularly in the USA, which may have impacted the emission ratio. However, without detailed information about the amount of gas and oil produced from all sources and their emission ratios, as a first approximation, we have used the mean ratio over the inversion period. We estimate the uncertainty in the optimized emissions due to the uncertainty in this ratio using Monte Carlo ensembles (described below). In addition, we include a sensitivity test in which the ratio is increased in one step to 0.175 after 2007 (see Text S4 and Figure S7). The other sources of CH_4 and C_2H_6 are treated as independent from one another.

Prior emissions estimates of CH_4 were compiled for each latitudinal box and each month using EDGAR-4.2 for anthropogenic sources (enteric fermentation and fugitive emissions from fossil fuels), the LPX-Bern land ecosystem model for wetlands, rice cultivation, and dry-soil oxidation (Spahni et al., 2013), Petrenko et al. (2017) for geological emissions, GFED-4.1s for biomass burning (van der Werf et al., 2010), Lambert and Schmidt (1993) for the ocean source, and Sanderson (1996) for emissions from termites (for prior emission values see Table S2). The emission estimates were resolved monthly and included interannual variations except for oceans and termites, which were only available as monthly climatologies. Since EDGAR-4.2 emissions are only available for 1970–2008 the emissions from 2008 were repeated for 2009 to 2014. For C_2H_6, the prior estimate for fossil fuel and geological emissions was based on that for CH_4 from EDGAR-4.2 and Petrenko et al. (2017) scaled by the ethane to methane emission ratio. The prior estimate for the other emissions category was based on GFED-4.1s for biomass burning and on the estimate of Etiope and Ciccioli (2009) for ocean emissions (a global climatological value; see Table S3). Our prior estimate for the global C_2H_6 source, of 22 Tg y^{-1}, is close to the recent estimate from Dalsøren et al. (2018) of 20 Tg y^{-1}.

The six CH_4 and two C_2H_6 sources, as well as the OH sink, were optimized in the inversion. Sources were optimized monthly for the four latitudinal boxes, and the OH sink in each box and month was optimized by scaling it globally and annually. Note that, although the (relatively minor) Cl sink is not optimized, its influence on the results was determined using sensitivity tests and its uncertainty is factored into the overall posterior uncertainty estimates (see next paragraph). For the inversion we used Bayesian inference to find the solution of maximum posterior probability (Rodgers, 2000). Details on the inversion method are given in Text S3, and a summary of the optimized variables is provided in Table S5.

A number of sensitivity tests were performed to assess the robustness of the results to changes in the source and sink uncertainties, to changes in the mean $\delta^{13}C_{CH4}$ value of fugitive emissions, to variations in the

strength of the Cl sink, and to an increase in the ethane to methane ratio after 2007 (see Text S4 and Figure S7). All tests gave consistent results, but the inversion that resulted in the closest fit to all observations (Test 3 in Table S7) was selected as the best scenario (from here on "reference" inversion). We estimate the posterior source uncertainty using a Monte Carlo ensemble to account for the uncertainties in the mean $\delta^{13}C_{CH4}$ values of the sources and sinks, as well as in the C_2H_6:CH_4 ratio (see Text S5). Furthermore, we used five additional Monte Carlo ensembles to determine which of the parameters (i.e., the $\delta^{13}C_{CH4}$ values and C_2H_6:CH_4 ratio) has the largest influence on the source uncertainty. The ensembles contained 500 members each and had a Gaussian distribution for the prior fluxes and $\delta^{13}C_{CH4}$ values and a truncated Gaussian distribution for the C_2H_6:CH_4 ratio (with truncation for the lower limit at 0.1).

3. Observational Data

We use monthly mean observations of CH_4 from the National Oceanic and Atmospheric Administration (NOAA) cooperative global air sampling network (Dlugokencky et al., 2009), $\delta^{13}C_{CH4}$ from the University of Colorado's Institute of Arctic and Alpine Research (INSTAAR) and the University of Washington's (UW) networks (Quay et al., 1999; White & Vaughn, 2015), and C_2H_6 from the University of California Irvine (UCI) and NOAA/INSTAAR networks (Blake, 2013; Helmig et al., 2011; Schultz et al., 2015). The reported uncertainties of the measurements are approximately 0.2% for CH_4, 3% for C_2H_6, and 0.1‰ for $\delta^{13}C_{CH4}$. Observations were used from sites that had quasi-continuous records (maps of all sites are shown in Figures S1–S3 in the supporting information). For C_2H_6, the UCI observations are available from 1984 and NOAA data start in 2005. Closely located sites from both networks were used to check for consistency during the overlapping period of 2005–2014. For $\delta^{13}C_{CH4}$, the UW observations are available until 1996 and INSTAAR data are available from 1998. The offset between these two laboratories' scales has been estimated to be 0.074‰ (based on the comparison with a third laboratory's measurements at Baring Head, New Zealand; Levin et al., 2012) and is less than the reported precision of approximately 0.1‰ (Miller et al., 2002; Quay et al., 1999).

Average mixing ratios of CH_4 and C_2H_6, and values of $\delta^{13}C_{CH4}$, were calculated for each lower tropospheric box and each month when observations were available. For the mean CH_4 mixing ratio for each box and month, observations from three sites were averaged (except for 0°–30°S where only two sites were available). For the mean $\delta^{13}C_{CH4}$ in each box and month, we used data from two sites (except 90°–30°N where four sites were available), and for C_2H_6 numerous sites were used to calculate the average for each box and month (see Figure S2). The greater number of sites used for the C_2H_6 averages was necessary owing to ethane's greater spatial variability owing to its shorter lifetime of ~60 days. The monthly mean data were filtered for outliers, defined as points outside 2-sigma standard deviations around the running mean. The total numbers of monthly averaged observations for CH_4, C_2H_6, and $\delta^{13}C_{CH4}$ were 1527, 836, and 1082, respectively.

4. Results

Figure 1 shows the interannual variations in the observed mixing ratios of CH_4, C_2H_6, and $\delta^{13}C_{CH4}$, along with the values modeled using the prior and posterior emissions from the reference inversion. (Note that the interannual variations shown here are calculated from the monthly observed and modeled values.) The prior emissions lead to large biases, especially in CH_4 and $\delta^{13}C_{CH4}$, whereas the posterior estimates reproduce the trends in CH_4, C_2H_6, and $\delta^{13}C_{CH4}$ comparatively well (see also Figures S4 to S6). The posterior emissions capture the period of near zero growth between 1998 and 2007 as well as the upward trend in CH_4 and downward trend in $\delta^{13}C_{CH4}$ from 2007. The total posterior CH_4 emission has a mean $\delta^{13}C_{CH4}$ value of -53.4 ± 5.0‰ (see Figure S7) and is enriched in ^{13}C compared to the prior (mean of -55.9 ± 7.6‰) but still has less ^{13}C relative to the atmosphere, which is enriched by the preferential loss of ^{12}C by OH and Cl oxidation. For C_2H_6, the posterior emissions reproduce the decreasing trend in the NH from the 1980s to the mid-1990s and its stabilization thereafter. In the NH, there is an observed increase in the annual mean mixing ratio of 23 ± 3 ppt y^{-1} from 2010 to 2014, as has previously been identified (Hausmann et al., 2016; Helmig et al., 2016), and is also captured by the posterior model with an increase of 20 ± 2 ppt y^{-1}. In general, the model has a low bias for C_2H_6, which could be due to a possible overestimate of C_2H_6 loss due to OH and/or Cl oxidation. Note also that the constraint from C_2H_6 is weaker owing to the higher uncertainty in the observation space for this species (~12.5% of the mean atmospheric value compared to ~0.5% and

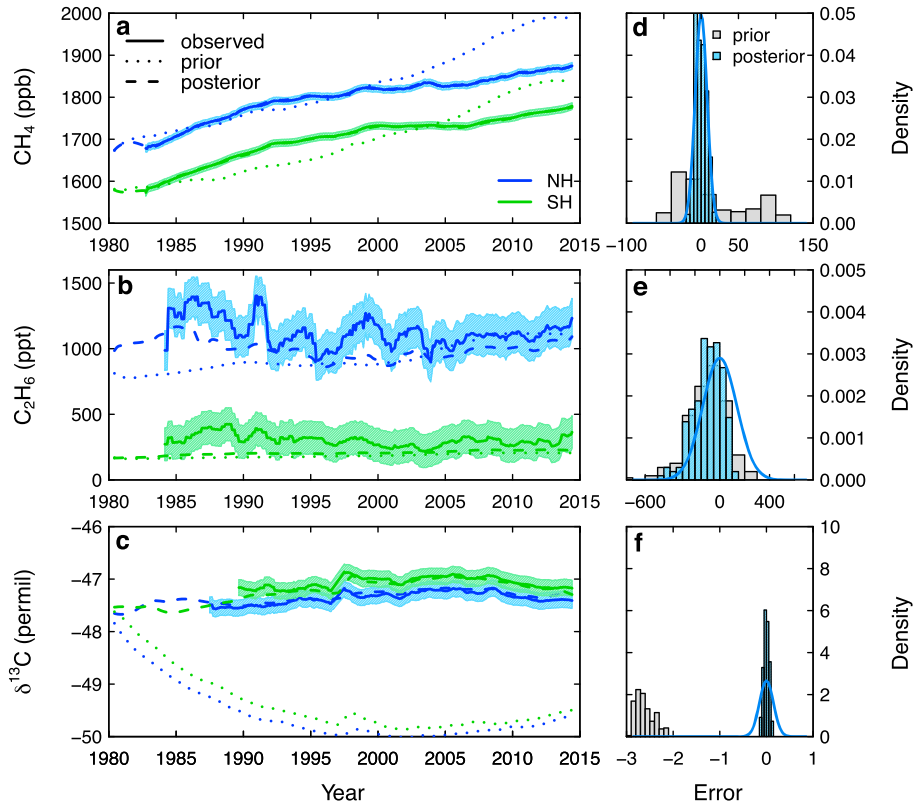

Figure 1. Annual trends in the Northern Hemisphere and Southern Hemisphere mean (a) CH_4 and (b) C_2H_6 mixing ratios and (c) $\delta^{13}C_{CH4}$. Note that for CH_4 the posterior curve (dashed line) lies directly on top of the observations. The annual trends were calculated by subtracting the monthly resolved seasonality (fitted using a 2-harmonic curve) and applying a 12-month running average to the residuals (the same procedure was applied to both the model and the observations). The shading indicates the observation uncertainty. Also shown are the distributions of the model-observation errors in the global monthly means (i.e., before subtracting the seasonality) of (d) CH_4 (in units of ppb), (e) C_2H_6 (in units of ppt), and (f) $\delta^{13}C$ (in units of per mil). The solid blue curve in (d) to (f) shows the *pdf* given by the observation uncertainty used in the inversion.

~0.3% for CH_4 and $\delta^{13}C_{CH4}$, respectively) to account for the larger measurement uncertainty and the uncertainty in the sink terms.

We focus the discussion of the results over the period 1985–2014, as prior to 1985 the observations are sparse, especially for C_2H_6 and $\delta^{13}C_{CH4}$. The global mean CH_4 emission for 1985–2014 found in our inversion was 505 ± 29 Tg y^{-1} and is close to the prior value of 525 ± 105 Tg y^{-1}. However, the trends are considerably different; the prior emissions increase steadily until 2010, while the optimized emissions have little trend until 2006 and then increase (see Figure S7). The inversion finds an increase in the global source of 43 ± 10 Tg y^{-1} between 2006 and 2014. Also noteworthy is the positive anomaly seen in 1997 owing to large biomass burning emissions associated with the strong El Niño event at this time (see Figure S8), as has previously been reported (Bousquet et al., 2006; Langenfelds et al., 2002). The OH sink increased from 429 ± 3 Tg y^{-1} in 1985 to 488 ± 4 Tg y^{-1} in 2014 approximately in proportion to the atmospheric CH_4 abundance. In contrast to the emissions, we found only small interannual variations in OH with small positive anomalies in 2004 and 2005 but fairly stable concentrations from 2007 (see Figure S9). Furthermore, the global CH_4 source and OH sink are robust against variations in the uncertainty assigned to the prior emissions and OH sink, as well as to the uncertainty in the mean $\delta^{13}C_{CH4}$ value of fossil fuel emissions (see Text S4 and Figures S7 and S9).

In our inversion, the global fossil fuel emission decreased by 14 ± 9 Tg y^{-1} from 1990 to 1996 but gradually increased again by 15 ± 8 Tg y^{-1} from 2006 to 2014. More recently, from 2010 to 2014, the inversion also found the C_2H_6 emissions to increase at a rate of 0.4 ± 0.3 Tg y^{-2}, which is consistent with the recent estimate of Helmig et al. (2016). The decrease in fossil fuel emissions in the 1990s is due to changes in the 90°–30°N box

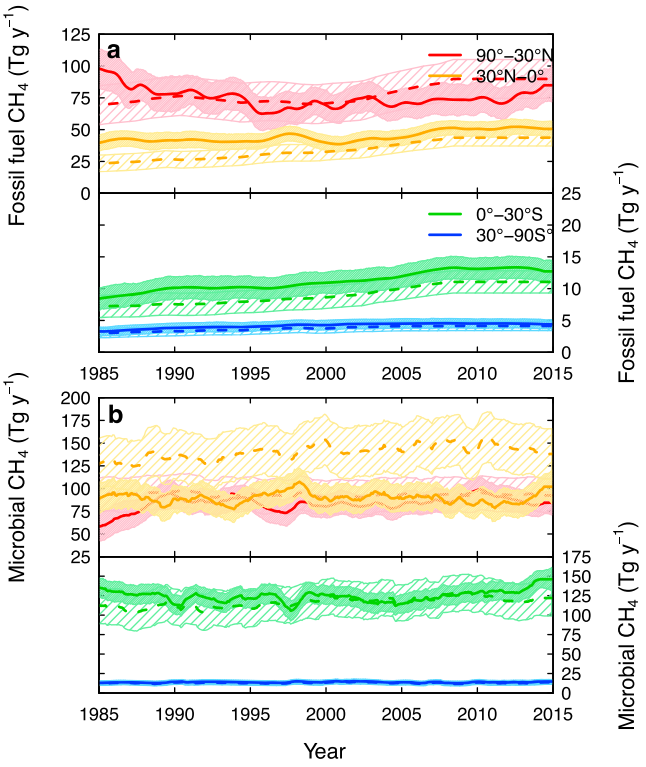

Figure 2. Annual trends in the (a) fossil fuel and (b) microbial CH_4 emissions for each of the latitudinal boxes. The annual trends were calculated by applying a 12-month running mean to the data. The dashed and solid lines show the prior and posterior emissions, and the diagonal and solid shaded areas indicate the prior and posterior uncertainties, respectively.

(Figure 2a). This result agrees well with previous studies, which point to a reduction in fossil fuel emissions in the early 1990s associated with the collapse of the Soviet Union and a subsequent large investment to reduce leaks associated with natural gas and oil production and distribution (Aydin et al., 2011; Bousquet et al., 2006; Dlugokencky et al., 1994, 2003; Simpson et al., 2012). In the late 1980s and early 1990s, an estimated 25–35 Tg y^{-1} of CH_4 was leaked to the atmosphere from Russia (Reshetnikov et al., 2000), but with the decline in production from 1991 to 1996, and likely reduction in leaks, the fugitive emission of CH_4 in the post-Soviet era dropped significantly, to an estimated 4 Tg y^{-1} (Dedikov et al., 1999). The estimated reduction from these bottom-up studies, of approximately 20–30 Tg y^{-1}, is larger than the mean estimate found by the inversion, but the lower estimate is still within the uncertainty range of the inversion result.

For the microbial source (which includes wetlands and enteric fermentation) the inversion finds significant interannual variations (Figure 2b), which explain up to 62% of the variation in the global CH_4 source. One notable change is the negative anomaly in the tropical and subtropical emissions in the SH during the 1997/1998 El Niño, as has previously been documented (Bousquet et al., 2006; Pison et al., 2013). In the inversion, the posterior microbial emissions in the SH tropics and subtropics (0°–30°S) decreased by 8.5 ± 7.0 Tg y^{-1} between 2000 and 2005. Previous atmospheric inversion studies have also found a decrease in tropical and subtropical microbial emissions during this period (Bousquet et al., 2006; Pison et al., 2013). From 2006 to 2014, we find a total increase in microbial emissions of 36 ± 12 Tg y^{-1}, which was mostly located in the tropics and subtropics. An increase in tropical and subtropical microbial emissions since 2006 has similarly been suggested in other recent studies (McNorton et al., 2016; Nisbet et al., 2016; Schaefer et al., 2016).

Since wetlands are the largest microbial source and are sensitive to changes in meteorology, particularly precipitation (which also influences wetland extent), we examined observed precipitation changes using the University of Delaware precipitation data set (https://www.esrl.noaa.gov/psd/data/gridded/data.UDel_AirT_Precip.html#detail). In subtropical and tropical wetland regions, where the largest changes were seen, we found a negative anomaly in precipitation from 2001 to 2005 and predominantly positive anomalies between 2006 and 2014, with the notable exception of the 2009/2010 El Niño (see Figure 3). There was a weak positive correlation between the tropical and subtropical microbial emissions and precipitation between 1996 and 2014 (R = 0.38) but significantly higher correlation between 1996 and 2005 (R = 0.61). The changes in the microbial emissions are consistent with what is expected from changes in a wetland source driven by precipitation anomalies (McNorton et al., 2016). However, it is unclear what is driving the strong increase in the microbial emissions between 2013 and 2014.

From our Monte Carlo ensembles, we calculated the posterior uncertainties for all sources and the OH sink, and their dependence on the uncertainties in the $\delta^{13}C_{CH4}$ values of the sources and the OH and Cl sinks, as well as the C_2H_6:CH_4 ratio. Taking into account all these contributions, the uncertainty reduction for the CH_4 emissions was approximately 40% for the microbial and 15% for the fossil fuel emissions and negligible for the remaining more minor sources. Overall uncertainties in the $\delta^{13}C_{CH4}$ values of the sources and sinks contributed similarly to the posterior uncertainty. The more minor sources were less well constrained and changed little compared to the prior estimates (<3 Tg y^{-1}) and similarly for the nonfossil fuel emissions of C_2H_6 (<0.2 Tg y^{-1}; see Figure S8). The soil oxidation loss of CH_4, however, was on average ~15 Tg y^{-1} smaller than the prior (Figure S8), but the uncertainty reduction for this source was negligible. Noteworthy is that the biomass burning emissions, though largely unchanged compared to the prior, decreased by 3.4 ± 1.7 Tg y^{-1} from 2006 to 2014, which is comparable to the result of Worden et al. (2017), who found a reduction in this source of 3.7 ± 1.4 Tg y^{-1} based on satellite retrievals of CH_4, CO, and fire activity.

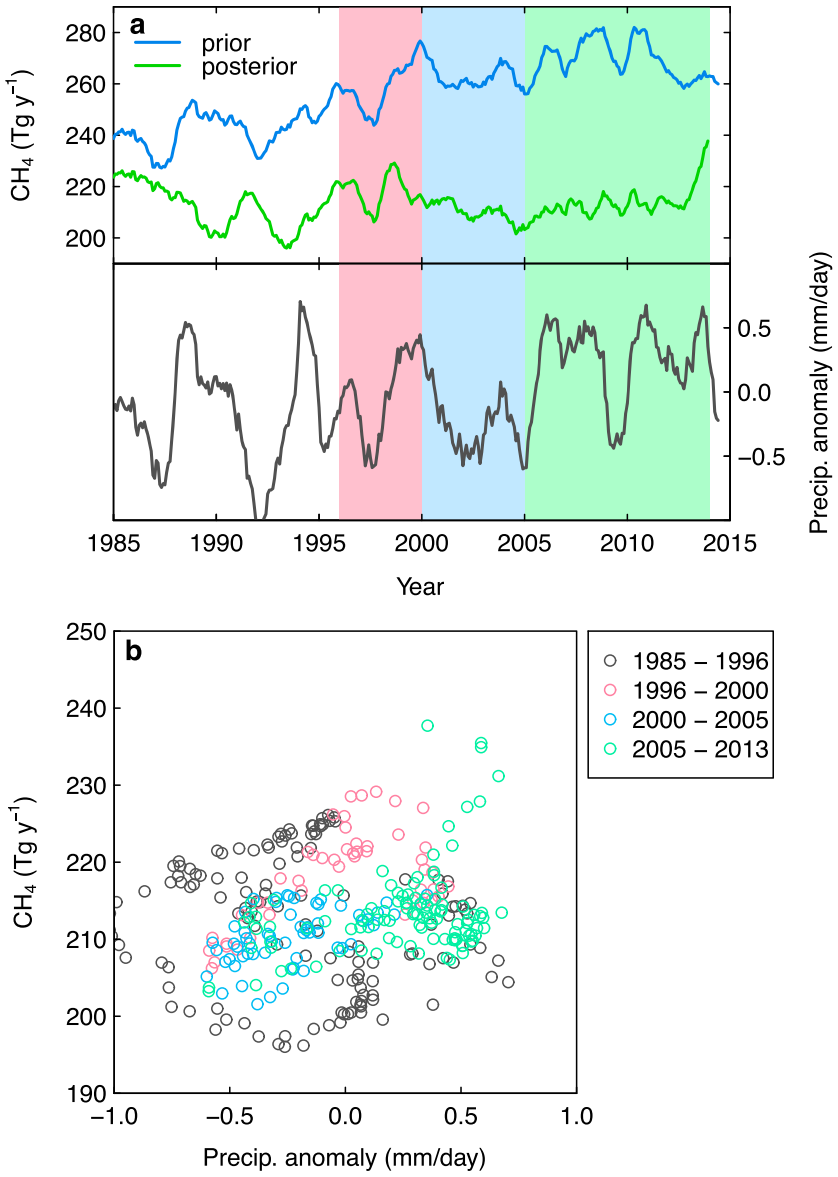

Figure 3. (a) Tropical and subtropical (30°N to 30°S) microbial emissions from the inversion (blue and green lines) and the area weighted mean precipitation rate anomaly in regions with >1% wetland area fraction in the tropics and subtropics (black line), (wetland area data from Poulter et al., 2017). The pink shading indicates the period 1996 to 2000, which includes the 1997/1998 El Niño; the blue shading indicates the period 2000 to 2005 when the posterior tropical and subtropical microbial emissions decreased; and the green shading indicates the period after 2005 when the posterior emissions increased again. (b) Also shown are the optimized tropical and subtropical microbial emissions versus the mean precipitation anomaly.

The decrease in the CH_4 growth rate from 1990 to 1996 is symptomatic of the budget approaching steady state as the global total emission ceased to increase in the late 1980s and actually decreased between 1990 and 1996 by 11 ± 9 Tg y^{-1}. This decrease was likely driven by a reduction in fossil fuel emissions of 14 ± 9 Tg y^{-1} but was partially offset by increases in other sources (Figure S11). The subsequent near-zero growth rate between 1998 and 2006 is owing to approximately stable total emissions, with changes in the fossil fuel emissions largely compensating those in the microbial emissions. Moreover, we find that the increase in CH_4 from ~1,779 ppb in 2007 to ~1,820 ppb in 2014 is driven by a net increase in the source of 43 ± 10 Tg y^{-1}, which is the balance of an increase in microbial and fossil fuel emissions of 36 ± 12 and

15 ± 8 Tg y^{-1}, respectively, a small decrease in biomass burning emissions of 3 ± 2 Tg y^{-1}, and an increase in soil oxidative loss of 5 ± 6 Tg y^{-1}.

5. Conclusions

We find that the increase in CH_4 from 2007 was largely driven by an increase in microbial emissions of 36 ± 12 Tg y^{-1}, predominantly in the tropics and subtropics, and fossil fuel emissions of 15 ± 8 Tg y^{-1}. In the tropics and subtropics, changes in the microbial emissions are broadly consistent with those expected from a wetland source responding to variations in precipitation. However, the period from 2005 to 2014 is only weakly correlated with precipitation anomaly; thus, other driving factors or contributions from other microbial sources, such as those from agriculture, likely also play a role. In addition, we find that the most likely explanation for the decline in the C_2H_6 mixing ratio, and a contributing factor in the decline of the CH_4 growth rate, from the late 1980s to the mid-1990s is a reduction in fossil fuel emissions of 14 ± 9 Tg y^{-1} (CH_4), which has probably occurred as a consequence of improvements in leak control in the oil and gas industries (Aydin et al., 2011).

Including C_2H_6, in supplement to CH_4 and $\delta^{13}C_{CH4}$, in the inversion provided an additional constraint on the fossil fuel source of CH_4 and thus indirectly on the other sources and, to some extent, also on the OH sink. Our results contrast with two recent studies that suggest that the increase in growth rate from 2007 may have been driven by a decrease in OH (Rigby et al., 2017; Turner et al., 2017), although we agree with their emphasis on the persisting large uncertainties in the CH_4 budget. Considering that the CH_4 increase is likely to be partially due to an increase in the fossil fuel source, there may be a possibility to curb the growth by mitigating these emissions.

Acknowledgments

NOAA CH_4 and C_2H_6 data are available from https://www.esrl.noaa.gov/gmd/dv/data/, INSTAAR $\delta^{13}C_{CH4}$ data from ftp://aftp.cmdl.noaa.gov/data/trace_gases/ch4c13/flask/, UW $\delta^{13}C_{CH4}$ data from http://cdiac.ornl.gov/ndps/quay.html (doi:10.3334/CDIAC/atg.026), and UCI C_2H_6 data from http://cdiac.ornl.gov/trends/otheratg/blake/blake.html. The modified version of the AGAGE 2-D model, the inversion code, and the optimized emissions are available on request to R.L.T. We kindly thank P. Quay (UW) for the use of the $\delta^{13}C_{CH4}$ data. R.L.T. and I.P. acknowledge the financial support of NordForsk to the eSTICC Nordic Centre of Excellence (grant 57001). E.G.N. was supported by the NERC Project MOYA (grant NE/N016211/1).

References

Allan, W., Struthers, H., & Lowe, D. C. (2007). Methane carbon isotope effects caused by atomic chlorine in the marine boundary layer: Global model results compared with Southern Hemisphere measurements. *Journal of Geophysical Research*, *112*, D04306. https://doi.org/10.1029/2006JD007369

Aydin, M., Verhulst, K. R., Saltzman, E. S., Battle, M. O., Montzka, S. A., Blake, D. R., et al. (2011). Recent decreases in fossil-fuel emissions of ethane and methane derived from firn air. *Nature*, *476*(7359), 198–201. https://doi.org/10.1038/nature10352

Blake, D. (2013). Methane, nonmethane hydrocarbons, alkyl nitrates, and chlorinated carbon compounds including 3 chlorofluorocarbons (CFC-11, CFC-12, and CFC-113) in whole-air samples. Oak Ridge, TN: Carbon Dioxide Information Analysis Center, Oak Ridge National The Laboratory, U.S. Department of Energy.

Bousquet, P., Ciais, P., Miller, J. B., Dlugokencky, E. J., Hauglustaine, D. A., Prigent, C., et al. (2006). Contribution of anthropogenic and natural sources to atmospheric methane variability. *Nature*, *443*(7110), 439–443. https://doi.org/10.1038/nature05132

Ciais, P., Sabine, C., Bala, G., Bopp, L., Brovkin, V., Canadell, J., et al. (2013). Chaper 6: Carbon and other biogeochemical cycles, IPCC WGI Fifth Assessment Report.

Cunnold, D. M., Steele, L. P., Fraser, P. J., Simmonds, P. G., Prinn, R. G., Weiss, R. F., et al. (2002). In situ measurements of atmospheric methane at GAGE/AGAGE sites during 1985–2000 and resulting source inferences. *Journal of Geophysical Research*, *107*(D14), 4225. https://doi.org/10.1029/2001JD001226

Dalsøren, S. B., Myhre, G., Hodnebrog, Ø., Myhre, C. L., Stohl, A., Pisso, I., et al. (2018). Discrepancy between simulated and observed ethane and propane levels explained by underestimated fossil emissions. *Nature Geoscience*, *11*(3), 178–184. https://doi.org/10.1038/s41561-018-0073-0

Dedikov, J. V., Akopova, G. S., Gladkaja, N. G., Piotrovskij, A. S., Markellov, V. A., Salichov, S. S., et al. (1999). Estimating methane releases from natural gas production and transmission in Russia. *Atmospheric Environment*, *33*(20), 3291–3299. https://doi.org/10.1016/S1352-2310(98)00388-4

Dlugokencky, E. J., Bruhwiler, L., White, J. W. C., Emmons, L. K., Novelli, P. C., Montzka, S. A., et al. (2009). Observational constraints on recent increases in the atmospheric CH4 burden. *Geophysical Research Letters*, *36*, L18803. https://doi.org/10.1029/2009GL039780

Dlugokencky, E. J., Houweling, S., Bruhwiler, L., Masarie, K. A., Lang, P. M., Miller, J. B., & Tans, P. P. (2003). Atmospheric methane levels off: Temporary pause or a new steady-state? *Geophysical Research Letters*, *30*(19), 1992. https://doi.org/10.1029/2003GL018126

Dlugokencky, E. J., Masaire, K. A., Lang, P. M., Tans, P. P., Steele, L. P., & Nisbet, E. G. (1994). A dramatic decrease in the growth rate of atmospheric methane in the Northern Hemisphere during 1992. *Geophysical Research Letters*, *21*(1), 45–48. https://doi.org/10.1029/93GL03070

Dlugokencky, E. J., Nisbet, E. G., Fisher, R., & Lowry, D. (2011). Global atmospheric methane: Budget, changes and dangers. *Philosophical Transactions of the Royal Society A: Mathematical, Physical and Engineering Sciences*, *369*(1943), 2058–2072. https://doi.org/10.1098/rsta.2010.0341

Etheridge, D. M., Steele, L., Francey, R. J., & Langenfelds, R. L. (1998). Atmospheric methane between 1000 AD and present: Evidence of anthropogenic emissions and climatic variability. *Journal of Geophysical Research*, *103*(D13), 15,979–15,993. https://doi.org/10.1029/98JD00923

Etiope, G., & Ciccioli, P. (2009). Earth's degassing: A missing ethane and propane source. *Science*, *323*(5913), 478. https://doi.org/10.1126/science.1165904

Gaubert, B., Worden, H. M., Arellano, A. F. J., Emmons, L. K., Tilmes, S., Barré, J., et al. (2017). Chemical feedback from decreasing carbon monoxide emissions. *Geophysical Research Letters*, *44*, 9985–9995. https://doi.org/10.1002/2017GL074987

Hausmann, P., Sussmann, R., & Smale, D. (2016). Contribution of oil and natural gas production to renewed increase in atmospheric methane (2007–2014): Top-down estimate from ethane and methane column observations. *Atmospheric Chemistry and Physics*, *16*(5), 3227–3244. https://doi.org/10.5194/acp-16-3227-2016

Helmig, D., Bottenheim, J., Galbally, I. E., Lewis, A., Milton, M. J. T., Penkett, S., et al. (2011). Volatile organic compounds in the global atmosphere. *Eos, Transactions American Geophysical Union*, *90*(52), 513–514. https://doi.org/10.1029/2009EO520001

Helmig, D., Rossabi, S., Hueber, J., Tans, P., Montzka, S. A., Masarie, K., et al. (2016). Reversal of global atmospheric ethane and propane trends largely due to US oil and natural gas production. *Nature Geoscience*, *9*(7), 490–495. https://doi.org/10.1038/ngeo2721

Hossaini, R., Chipperfield, M. P., Saiz-Lopez, A., Fernandez, R., Monks, S., Feng, W., et al. (2016). A global model of tropospheric chlorine chemistry: Organic versus inorganic sources and impact on methane oxidation. *Journal of Geophysical Research: Atmospheres*, *121*, 14,271–14,297. https://doi.org/10.1002/2016JD025756

Jones, V. T., Matthews, M. D., & Richers, D. M. (1999). Light hydrocarbons for petroleum and gas prospecting. *Handbook of Exploration Geochemistry*, *7*, 133–212.

Kirschke, S., Bousquet, P., Ciais, P., Saunois, M., Canadell, J. G., Dlugokencky, E. J., et al. (2013). Three decades of global methane sources and sinks. *Nature Geoscience*, *6*(10), 813–823. https://doi.org/10.1038/ngeo1955

Kort, E. A., Smith, M. L., Murray, L. T., Gvakharia, A., Brandt, A. R., Peischl, J., et al. (2016). Fugitive emissions from the Bakken shale illustrate role of shale production in global ethane shift. *Geophysical Research Letters*, *43*, 4617–4623. https://doi.org/10.1002/2016GL068703

Krol, M., Houweling, S., Bregman, B., Broek, V. D. M., Segers, A., Velthoven, P. V., et al. (2005). The two-way nested global chemistry-transport zoom model TM5: Algorithm and applications. *Atmospheric Chemistry and Physics*, *5*(2), 417–432. https://doi.org/10.5194/acp-5-417-2005

Lambert, G., & Schmidt, S. (1993). Reevaluation of the oceanic flux of methane: Uncertainties and long term variations. *Chemosphere*, *26*(1-4), 579–589. https://doi.org/10.1016/0045-6535(93)90443-9

Langenfelds, R., Francey, R., Pak, B. C., Steele, L. P., Lloyd, J., Trudinger, C. M., & Allison, C. E. (2002). Interannual growth rate variations of atmospheric CO_2 and its delta13C, H_2, CH_4, and CO between 1992 and 1999 linked to biomass burning. *Global Biogeochemical Cycles*, *16*(3), 1048. https://doi.org/10.1029/2001GB001466

Levin, I., Veidt, C., Vaughn, B. H., Brailsford, G., Bromley, T., Heinz, R., et al. (2012). No inter-hemispheric δ13CH4 trend observed. *Nature*, *486*(7404), E3–E4. https://doi.org/10.1038/nature11175

Liang, Q., Chipperfield, M. P., Fleming, E. L., Abraham, N. L., Braesicke, P., Burkholder, J. B., et al. (2017). Deriving global OH abundance and atmospheric lifetimes for long-lived gases: A search for CH_3CCl_3 alternatives. *Journal of Geophysical Research: Atmospheres*, *122*, 11,914–11,933. https://doi.org/10.1002/2017JD026926

McNorton, J., Gloor, E., Wilson, C., Hayman, G. D., Gedney, N., Comyn-Platt, E., et al. (2016). Role of regional wetland emissions in atmospheric methane variability. *Geophysical Research Letters*, *43*, 11,433–11,444. https://doi.org/10.1002/2016GL070649

Miller, J. B., Mack, K. A., Dissly, R., White, J. W., Dlugokencky, E. J., & Tans, P. P. (2002). Development of analytical methods and measurements of $^{13}C/^{12}C$ in atmospheric CH_4 from the NOAA climate monitoring and diagnostics laboratory global air sampling network. *Journal of Geophysical Research*, *107*(D13), 4178. https://doi.org/10.1029/2001JD000630

Montzka, S. A., Dutton, G. S., Yu, P., Ray, E., Portmann, R. W., Daniel, J. S., et al. (2018). An unexpected and persistent increase in global emissions of ozone-depleting CFC-11. *Nature*, *557*(7705), 413–417. https://doi.org/10.1038/s41586-018-0106-2

Montzka, S. A., Krol, M., Dlugokencky, E., Hall, B., Jöckel, P., & Lelieveld, J. (2011). Small interannual variability of global atmospheric hydroxyl. *Science*, *331*(6013), 67–69. https://doi.org/10.1126/science.1197640

Nisbet, E. G., Dlugokencky, E. J., & Bousquet, P. (2014). Methane on the rise—Again. *Science*, *343*(6170), 493–495. https://doi.org/10.1126/science.1247828

Nisbet, E. G., Dlugokencky, E. J., Manning, M. R., Lowry, D., Fisher, R. E., France, J. L., et al. (2016). Rising atmospheric methane: 2007–2014 growth and isotopic shift. *Global Biogeochemical Cycles*, *30*, 1356–1370. https://doi.org/10.1002/2016GB005406

Petrenko, V. V., Smith, A. M., Schaefer, H., Riedel, K., Brook, E., Baggenstos, D., et al. (2017). Minimal geological methane emissions during the Younger Dryas-Preboreal abrupt warming event. *Nature*, *548*(7668), 443–446. https://doi.org/10.1038/nature23316

Pison, I., Ringeval, B., Bousquet, P., Prigent, C., & Papa, F. (2013). Stable atmospheric methane in the 2000s: Key-role of emissions from natural wetlands. *Atmospheric Chemistry and Physics*, *13*(23), 11,609–11,623. https://doi.org/10.5194/acp-13-11609-2013

Poulter, B., Bousquet, P., Canadell, J. G., Ciais, P., Peregon, A., Saunois, M., et al. (2017). Global wetland contribution to 2000–2012 atmospheric methane growth rate dynamics. *Environmental Research Letters*, *12*(9), 094013. https://doi.org/10.1088/1748-9326/aa8391

Quay, P., Stutsman, J., Wilbur, D., Snover, A., Dlugokencky, E., & Brown, T. (1999). The isotopic composition of atmospheric methane. *Global Biogeochemical Cycles*, *13*(2), 445–461. https://doi.org/10.1029/1998GB900006

Reshetnikov, A. I., Paramonova, N. N., & Shashkov, A. A. (2000). An evaluation of historical methane emissions from the Soviet gas industry. *Journal of Geophysical Research*, *105*(D3), 3517–3529. https://doi.org/10.1029/1999JD900761

Rice, A. L., Butenhoff, C. L., Teama, D. G., Röger, F. H., Khalil, M. A. K., & Rasmussen, R. A. (2016). Atmospheric methane isotopic record favors fossil sources flat in 1980s and 1990s with recent increase. *Proceedings of the National Academy of Sciences of the United States of America*, *113*(39), 10,791–10,796. https://doi.org/10.1073/pnas.1522923113

Rigby, M., Montzka, S. A., Prinn, R. G., White, J. W. C., Young, D., O'Doherty, S., et al. (2017). Role of atmospheric oxidation in recent methane growth. *Proceedings of the National Academy of Sciences of the United States of America*, *114*(21), 5373–5377. https://doi.org/10.1073/pnas.1616426114

Rodgers, C. D. (2000). *Inverse methods for atmospheric sounding: Theory and practice*. Singapore: World Scientific. https://doi.org/10.1142/3171

Rudolph, J. (1995). The tropospheric distribution and budget of ethane. *Journal of Geophysical Research*, *100*(D6), 11,369–11,381. https://doi.org/10.1029/95JD00693

Sanderson, M. G. (1996). Biomass of termites and their emissions of methane and carbon dioxide: A global database. *Global Biogeochemical Cycles*, *10*(4), 543–557. https://doi.org/10.1029/96GB01893

Saunois, M., Bousquet, P., Poulter, B., Peregon, A., Ciais, P., Canadell, J. G., et al. (2017). Variability and quasi-decadal changes in the methane budget over the period 2000–2012. *Atmospheric Chemistry and Physics*, *17*(18), 11,135–11,161. https://doi.org/10.5194/acp-17-11135-2017

Schaefer, H., Fletcher, S. E., Veidt, C., Lassey, K. R., Brailsford, G. W., Bromley, T. M., et al. (2016). A 21st century shift from fossil-fuel to biogenic methane emissions indicated by $^{13}CH_4$. *Science*, *352*(6281), 80–84. https://doi.org/10.1126/science.aad2705

Schultz, M. G., Akimoto, H., Bottenheim, J., Buchmann, B., Galbally, I. E., Gilge, S., et al. (2015). The global atmosphere watch reactive gases measurement network. *Elementa: Science of the Anthropocene*, *3*, 1–24. https://doi.org/10.12952/journal.elementa.000067

Schwietzke, S., Griffin, W. M., Matthews, H. S., & Bruhwiler, L. M. (2014). Global bottom-up fossil fuel fugitive methane and ethane emissions inventory for atmospheric modeling. *ACS Sustainable Chemistry & Engineering*, *2*(8), 1992–2001. https://doi.org/10.1021/sc500163h

Schwietzke, S., Sherwood, O. A., Bruhwiler, L. M. P., Miller, J. B., Etiope, G., Dlugokencky, E. J., et al. (2016). Upward revision of global fossil fuel methane emissions based on isotope database. *Nature*, *538*(7623), 88–91. https://doi.org/10.1038/nature19797

Simpson, I. J., Sulbaek Andersen, M. P., Meinardi, S., Bruhwiler, L., Blake, N. J., Helmig, D., et al. (2012). Long-term decline of global atmospheric ethane concentrations and implications for methane. *Nature*, *488*(7412), 490–494. https://doi.org/10.1038/nature11342

Smith, M. L., Kort, E. A., Karion, A., Sweeney, C., Herndon, S. C., & Yacovitch, T. I. (2015). Airborne ethane observations in the Barnett shale: Quantification of ethane flux and attribution of methane emissions. *Environmental Science & Technology*, *49*(13), 8158–8166. https://doi.org/10.1021/acs.est.5b00219

Spahni, R., Joos, F., Stocker, B. D., Steinacher, M., & Yu, Z. C. (2013). Transient simulations of the carbon and nitrogen dynamics in northern peatlands: From the Last Glacial Maximum to the 21st century. *Climate of the Past*, *9*(3), 1287–1308. https://doi.org/10.5194/cp-9-1287-2013

Strępoć, D., Mastalerz, M., Eble, C., & Schimmelmann, A. (2007). Characterization of the origin of coalbed gases in southeastern Illinois Basin by compound-specific carbon and hydrogen stable isotope ratios. *Organic Geochemistry*, *38*(2), 267–287. https://doi.org/10.1016/j.orggeochem.2006.09.005

Turner, A. J., Frankenberg, C., Wennberg, P. O., & Jacob, D. J. (2017). Ambiguity in the causes for decadal trends in atmospheric methane and hydroxyl. *Proceedings of the National Academy of Sciences of the United States of America*, *114*(21), 5367–5372. https://doi.org/10.1073/pnas.1616020114

van der Werf, G. R., Randerson, J. T., Giglio, L., Collatz, G. J., Mu, M., Kasibhatla, P. S., et al. (2010). Global fire emissions and the contribution of deforestation, savanna, forest, agricultural, and peat fires (1997–2009). *Atmospheric Chemistry and Physics*, *10*(23), 11,707–11,735. https://doi.org/10.5194/acp-10-11707-2010

White, J. W. C., & Vaughn, B. H. (2015). University of Colorado, Institute of Arctic and Alpine Research (INSTAAR), stable isotopic composition of atmospheric methane (^{13}C) from the NOAA ESRL Carbon Cycle Cooperative Global Air Sampling Network, 1998–2014, version: 2015-08-03.

Worden, J. R., Bloom, A. A., Pandey, S., Jiang, Z., Worden, H. M., Walker, T. W., et al. (2017). Reduced biomass burning emissions reconcile conflicting estimates of the post-2006 atmospheric methane budget. *Nature Communications*, *8*(1), 2227. https://doi.org/10.1038/s41467-017-02246-0